Antiproton identification with BESS-Polar II Aerogel Cherenkov Counter

K. Sakai*, **T. Hams**†, **M. Hasegawa**‡, **K. Yoshimura**‡, **K. Abe**§, **H. Fuke**¶, **S. Haino**‡, **A. Horikoshi**‡, **K. C. Kim**‖, **T. Kumazawa**‡, **A. Kusumoto**§, **M-H. Lee**‖, **Y. Makida**‡, **S. Matsuda**‡, **Y. Matsukawa**§, **J. W. Mitchell**†, **A. A. Moiseev**†, **J. Nishimura***, **M. Nozaki**‡, **R. Orito**§, **J. F. Ormes****, **M. Sasaki**†, **E. S. Seo**‖, **Y. Shikaze**§, **R. Shinoda***, **R. E. Streitmatter**†, **J. Suzuki**‡, **K. Takeuchi**§, **N. Thakur****, **K. Tanaka**‡, **T. Yamagami**¶, **A. Yamamoto**‡ **and T. Yoshida**¶

**The University of Tokyo, Bunkyo, Tokyo 113-0044, Japan*
†NASA Goddard Space Flight Center (NASA/GSFC), Greenbelt, MD 20771, USA
‡High Energy Accelerator Research Organization (KEK), Oho, Tsukuba, Ibaraki 305-0801, Japan
§Kobe University, Kobe, Hyogo 657-850, Japan
¶ Institute of Space and Astronautical Science, Japan Aerospace Exploration Agency (ISAS/JAXA), Sagamihara, Kanagawa 229-8510, Japan
‖University of Maryland, College Park, MD 20742, USA
***University of Denver, Denver, CO 80208, USA*

***Abstract*. The Balloon-borne Experiment with a Superconducting Spectrometer (BESS experiment) had two successful flights over Antarctica in 2004/12 and 2007/12. The experiment is designed to precisely measure the antiproton spectrum in the galactic cosmic radiation studying elementary particle phenomena in the early universe and searching for novel cosmological primary antiproton sources. Two methods were used to achieve background-free and mass-identified detection of antiprotons up to 3 GeV. One method was a threshold type Aerogel Cherenkov counter (ACC), which eliminates the overwhelming e-/μ- background. The ACC used in first BESS-Polar flight (BESS-Polar I), however, did not have enough light yield and thus insufficient performance, resulting in residual e-/μ- background contaminating the antiproton sample. To achieve unprecedented sensitivity for the antiproton flux combined with the higher statistics ($\sim 5 \times 10^9$ events) expected in BESS-Polar II, a new ACC has been developed employing larger size aerogel blocks. The design was optimized by various studies using test beam results, and Monte-Carlo simulation of the light-diffusion box configuration considering the magnetic field constraints on the fine-mesh photomultiplier tubes (PMT). As a result, the effective mean number of photoelectrons (N.pe.) obtained in BESS-Polar II was determined to be 11.3, which is twice the light yield of the BESS-Polar I ACC. In this paper, the antiproton identification with the improved ACC of BESS-Polar II will be presented.**

***Keywords*: BESS-Polar II, Cosmic-ray antiproton, Aerogel Cherenkov counter**

I. Introduction

The BESS experiment has precisely measured spectra of antiprotons to study elementary particle phenomena in the early universe and has searched for antiprotons of novel cosmic origins[1,2,3,4].

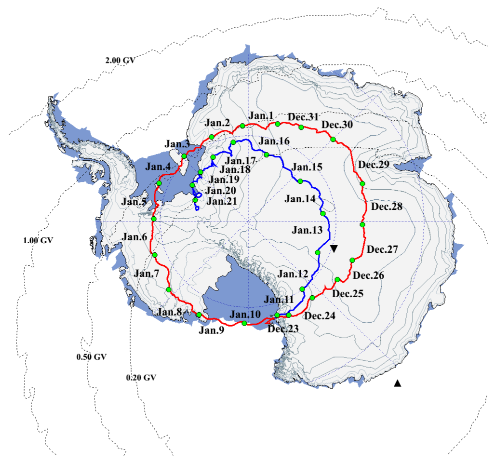

Fig. 1. Flight trajectory of the 2007 BESS-Polar II over Antarctica from Williams Field.
[Launch]S77-51,E166-40, 06:27(McM) 12/23 2007
[Recovery]S83-51,W073-04, 09:02(UTC) 1/21 2008

Two long-duration flights from Antarctica were carried out using an upgraded BESS spectrometer (BESS-Polar) designed for an extremely sensitive search for low energy cosmic-ray antiprotons. The first scientific flight of the BESS-Polar I payload was launched near McMurdo Station, on December 13th, 2004 (UTC). The flight duration was over 8.5 days and more than 9×10^8 cosmic-ray events were recorded[5,6]. Overall, the first flight and observation of BESS-Polar was successful, but two technical issues needed to the addressed for the second main science flight of BESS-Polar:(1) eliminate the excessive high-voltage current in some of the Time-of-Flight (TOF) PMT and (2) increase the background rejection power of the Aerogel Cherenkov Counter. Both

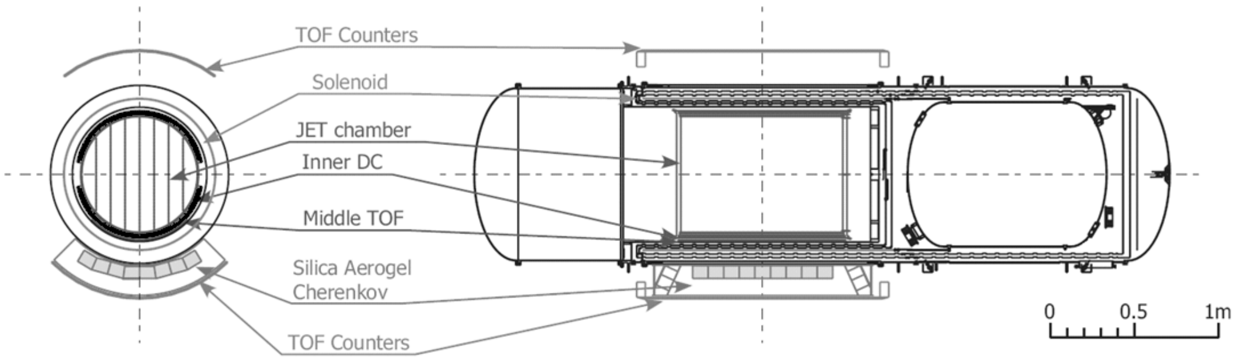

Fig. 2. Cross-sectional views of the BESS-Polar II payload

improvements were successfully implemented for, the second scientific flight of BESS-Polar II realized on December 23rd, 2007 (UTC) at solar minimum[7]. The flight duration was 29 days of which the first 24.5 days were for scientific observation, limited by the cryogenic life-time of the magnet, recording over 47×10^8 cosmic-ray events [Fig 1]. In this paper, we will report on the improvements to the ACC. The improvements to the TOF system are discussed elsewhere in these proceedings.

II. Detector description

The BESS-Polar II spectrometer, shown in Fig.2, consists of a superconducting solenoid magnet (MAG), a drift chamber tracking system (JET/IDC), a three layer TOF scintillator hodoscopes, a silica-aerogel Cherenkov counter (ACC), a data acquisition system (DAQ), and a photovoltaic array as power supply. Although the detector concept is very similar, the BESS-Polar II experiment had the following important improvements over BESS-Polar I.

- Higher Statistics due to longer cryogenic lift-time of magnet
- Unique opportunity to measure low energy flux at Solar minimum
- Lower systemactic errors due to improved efficiencies in the particle identification and the data acquisition system

III. Aerogel Chrenkov Counter

A high sensitivity in the antiproton search with the BESS-Polar instrument requires a large rejection factor in the threshold-type Aerogel Cherenkov counter, which is capable of removing the overwhelming light e-/μ- background from the antiproton sample.

The BESS-Polar I ACC had a marginally sufficient background rejection factor and some e-/μ- events remained as background in the antiproton sample resulting in an increased systematic error in the antiproton flux. To obtain the antiproton flux with unprecedented sensitivity and higher statistics, a new ACC for BESS-Polar II was developed.

IV. Development of ACC

We will discuss the three areas that were studied to improve the ACC for BESS-Polar II. The areas are as follows:

A) Increase aerogel block size and improve their optical properties
B) Optimize the geometry of light-diffusion box
C) Optimize the photosensitive area of th PMT in the presence of the magnetic field

A. Production of Silica Aeorgel Block

As for the BESS-Polar I, the silica Aerogel Cherenkov radiator was acquired from Matsushita Electric Works in Japan. In contrast to BESS-Polar I, Matsushita Electric Works had improved their manufacturing capabilities and was able to provide significantly larger aerogel pieces, which reduced the number of aerogel block interfaces in the counter volume. Particles passing through the interface regions between adjacent aerogel blocks need to be eliminated from the data due to their potential

TABLE I
Feature of aerogel blocks

	Polar-I Aerogel	Polar-II Aerogel
Block size	$100 \times 100 \times 80$ mm	$190 \times 280 \times 80$ mm
Refraction factor	1.02	1.03
Identification region	~ 3.8 GeV	~ 3.0 GeV
Required number	72 blocks	12 blocks

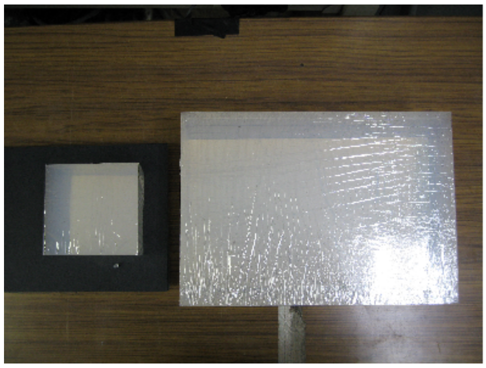

Fig. 3. Comparison aerogel block. Left block was used in Polar-I and right block was reproduced for Polar-II.

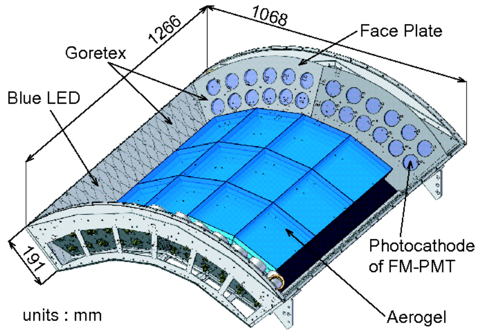

Fig. 4. Overview of the Aerogel Cherenkov counter.

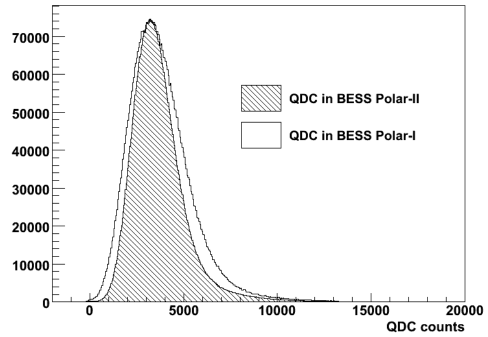

Fig. 5. QDC distribution of ACC.

reduced light yield. Larger radiator blocks also reduced the amount of absorption in the UV-transparent PET film, which held the aerogel pieces in place. For BESS-Polar II the refractive index of the aerogel was increased from 1.02 to 1.03 yielding 1.5 times more light.

B. *Structure optimization using MC simulation*

An intensive study using a GEANT4 Monte-Carlo simulation of the ACC light yield was undertaken to improve the light collection of the counter. The optical parameters of the aerogel were derived from a beam test at KEK in which a number of different ACC configuration were tested. Fig. 4 shows a schematic view of the final design. The counter consists of a large diffusion box containing the aerogel blocks, which are viewed by 48 PMTs densely arranged at both the ends. The weight of the counter and the amount of material in the path of the particle were minimized using a rigid isogrid outer frame and thin carbon-fiber composite windows as light closeouts. The interior of the counter volume is lined with highly reflective Gore-Tex, which exhibits high reflectivity of $> 90\%$ even in the short-wavelength region (300 - 400 nm).

C. *PMTs' configuration*

The photon detector viewing the cherenkov radiator have to operate in a 0.2T fringe field from the magnet. We selected the 2.5 inch diameter fine-mesh type PMTs (R6504, Hamamatsu Photonics K. K.) whose sensitive region lies between 300 and 700 nm. These PMTs were selected for their high tolerance for axially aligned magnetic fields. But because the magnetic field can not be fully aligned for all PMT simultaneously by a single mounting plate tilt angle (see Fig. 4), some PMT will be slightly misaligned. A misalignment of a PMT with a non-axial magnetic field will cause a loss of effective photocathode area (S_{eff}), i.e., some secondary electrons produced at a dynode cannot reach the anode, because they are deflected by the magnetic field. The detector configuration has been optimized to maximize the total effective sensitive area, S_{eff}, which was found at a tilt angle of 31.1°. To calibrate and adjust the PMT gain in the magnetic inside the counter, a blue LED with a peak emission at 450 nm is mounted on either the sides of the side plate at its center point.

TABLE II
PHYSICAL PARAMETERS FOR MONTE CARLO MC

	Setting value
Scattering length of Aerogel Block	$\Lambda_{scatter} = \lambda^4/C$
Absorption length	$\Lambda_{abs} = 16.2cm$ $(\lambda > 420mm)$
Reflectance of Gore-Tex	97 %

V. PERFORMANCE

Pre-flight, the counter performance was evaluated using cosmic-ray data collected with the BESS Polar-II configuration. During the 24.5 day long flight, all but one of the 48 PMT in the ACC were working correctly. The one PMT had to be turned off since it had a sudden large current increase and became unstable.

A. *Light yield*

Fig. 5 shows the charge sum (QDC) distribution collected from all PMT signals for high momentum protons events (RGT $>$ 20 GV) passing through the center of the ACC. By fitting data in region 0 - 10000 counts to a Poisson distribution, the effective mean number of Photoelectrons (N.pe.) is determined to be 11.3. This value is consistent with the expected design value estimated by following equation.

$$\text{N.pe.} = 6.7_{(1)} \times 1.47_{(2)} \times 1.1_{(3)} \times 1.1_{(4)} = 11.9(\text{design})$$

1) N.pe. of BESS Polar-I
2) Effect of Refractive factor change ($1.02 \rightarrow 1.03$)
3) Effect of Structure optimization
4) Effect of Aerogel blocks' size change

The increased amount of Cherenkov light collected in ACC is directly related to the performance improvements in BESS-Polar II ACC rejection power.

B. *Background Rejection*

Fig. 6 shows the inverse velocity versus Rigidity plots for single charged particle surviving the standard selection in BESS-Polar II. As shown here, the e- and μ- background start to contaminate the $\bar{p}$ band around $\beta^{-1} \leq 1.1$ [Left figure in Fig. 6]. The right figure shows

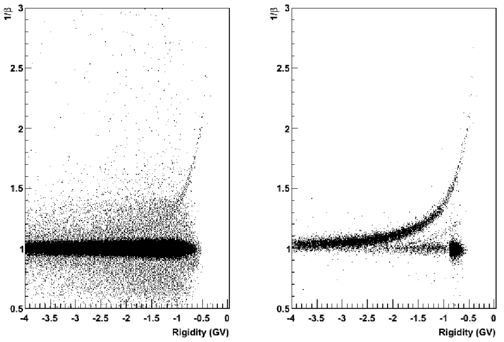

Fig. 6. β^{-1} vs Rigidity plots in BESS-Polar II. Left figure is before aerogel Chrenkov cut and right is after cut.

the β^{-1} versus R plot for same data set, but in addition a Cherenkov veto, requiring no light signal, is also imposed. The lighter e- and μ- are already relativistic at these rigidities and produce Cherenkov light and are removed. Using the combination of the Cherenkov veto and excellent velocity (β^{-1}) resolution of the TOF, the $\bar{p}$ candidates can be mass-identified up to 3.8 GV, which is the onset of the Cherenkov effect for $\bar{p}$.

VI. Antiproton identification

Particle mass are related o rigidity, R, velocity, β, and charge, Z, as;

$$m = ZeR\sqrt{1/\beta^2 - 1}$$

The particle charge, $|Z|$, is determined by the energy loss, dE/dx, band in the TOF and the JET chamber. After selection of $|Z| = 1$ particles with dE/dx band, antiprotons, $\bar{p}$, can be identified as a mass band in the particle identification plot (β^{-1} vs. R). The solid lines in Figure 7 represent boundaries of β band cut for the antiproton selection. Finally we see a clear narrow band of about 8×10^3 $\bar{p}$ candidates for BESS-Polar II data.

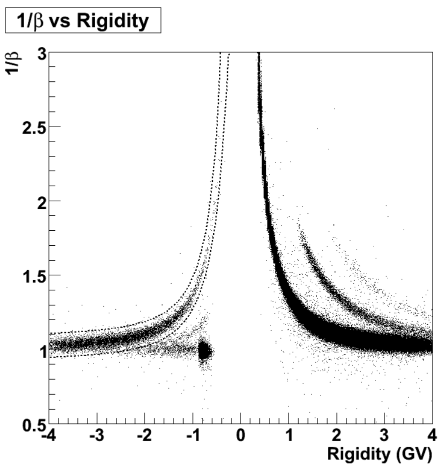

Fig. 7. β^{-1} vs Rigidity plots in the BESS-Polar II flight after all event selection.

TABLE III
Progress of BESS ballon flights and observations

Experiment	Number of $\bar{p}$ candidates
BESS-93	6
BESS-94	2
BESS-95	43*
BESS-97	415*
BESS-98	398
BESS-99	668
BESS-00	558
BESS-TeV ('01)	147
BESS-Polar I ('04)	1512
BESS-Polar II ('07)	> 8000*

($*$: Data in Solar minimum)

The number of $\bar{p}$ candidates in BESS-Polar II is about 20 times the statistics in previous solar minimum period $(95 + 97)$ see a summary in Table III.

VII. Summary and conclusions

We have described the development of the aerogel Cherenkov counter employed in the BESS-Polar II experiment. This counter features a large sensitive area, sufficient flight durability, and good performance in a magnetic field of 0.2 T. The BESS-Polar II ACC demonstrated a mean number of 11.3 photoelectrons in flight, which is almost twice the value in BESS-Polar I (= 6.7). Based on the improved photoelectron statistics in the BESS-Polar II ACC, we expect a e-/μ- rejection power 10 times higher than achieved with the BESS-Polar I ACC.

Acknowledgements

The authors thank NASA Headquarters for the continuous encouragement in this U.S.-Japan cooperative project. Sincere thanks are expressed to the NASA Balloon Programs Office at GSFC/WFF and CSBF for their experienced support. They also thank ISAS/JAXA and KEK for their continuous support and encouragement. Special thanks go to the National Science Foundation (NSF), U.S.A., and Raytheon Polar Service Company for their professional support in U.S.A. and in Antarctica. The BESS-Polar experiment is being carried out as a Japan-U.S. collaboration, and is supported by a KAKENHI(13001004 and 18104006) in Japan, and by NASA in U.S.A.

References

[1] A. Yamamoto et al., Adv.Res 14 (1994) no.2, 75
[2] S. Orito et al., Phys.Rev.Lett 84 (2000) 1078
[3] Y. Ajima et al., Nucl. Instr. Methods A 443 (2000) 71
[4] A. Yamamoto et al., Adv. Space Res. 30 (2002) no.1253
[5] A. Yamamoto et al., Adv. Space Res, 42 (2008) no.442
[6] K. Abe et al., Phys. Lett B 670 (2008) 103
[7] K. Yoshimura et al., Adv.Space Res. 42(2008) no.1664